7144 *Inorg. Chem.* **2010**, *49*, 7144–7155
DOI: 10.1021/ic100960z

Inorganic Chemistry
Article

Highly Volatile Alkaline Earth Metal Fluoroalkoxides

William D. Buchanan, Marites A. Guino-o, and Karin Ruhlandt-Senge*

Department of Chemistry, 1-014 Center for Science and Technology, Syracuse University, Syracuse, New York 13244-4100

Received May 14, 2010

The synthetic strategies, structural comparison, and thermal gravimetric analyses for a novel family of alkaline earth metal perfluoro-*tert*-butoxides (PFTB) are presented. The isolated complexes follow the general formula, $[Ae(PFTB)_2(d)_x]$; (**1a**, Ae = Mg, d = THF, $x = 2$; **1b**, Ae = Ca, d = THF, $x = 4$; **1c**, Ae = Sr, d = THF, $x = 4$; **1d**, Ae = Ba, d = THF, $x = 4$; **2a**, Ae = Mg, d = DME, $x = 1$; **2b**, Ae = Ca, d = DME, $x = 2$; **2c**, Ae = Sr, d = DME, $x = 2$; **2d**, Ae = Ba, d = DME, $x = 3$; **3a**, Ae = Mg, d = diglyme, $x = 1$; **3b**, Ae = Ca, d = diglyme, $x = 2$; **3c**, Ae = Sr, d = diglyme, $x = 2$; **3d**, Ae = Ba, d = diglyme, $x = 2$; THF = tetrahydrofuran, DME = 1,2-dimethoxyethane) where the crystallographically characterized compounds display either a *cis* or *trans* conformations in octahedral or pseudo-octahedral environments. Alkane elimination (Mg), direct metalation via ammonia activation (Ca, Sr, Ba), and transamination (Ca, Sr, Ba) methods yielded the target compounds in moderate to good yields. Structural studies of select compounds showed all compounds to be monomeric with varying degrees of co-ligand coordination, possibly explaining some of the observed physical properties. Thermal gravimetric analyses of the compounds shows sublimation at low temperatures, associated with minimal residue, making this family of fluoroalkoxides promising candidates for metal organic chemical vapor deposition (MOCVD).

1. Introduction

Highly volatile metal organic chemical vapor deposition (MOCVD) precursors of alkaline earth metal complexes remain the focus of intense research for application in the production of semi- and superconductors. Many MOCVD efforts focus on producing high quality $YBa_2Cu_3O_{7-x}$[1] films; however, other materials based on $BaTiO_3$,[2] BiSrCaCuO,[3] and alkaline earth-fluorides[4,5] are also attractive targets . A wide variety of potential precursors have been examined, bearing ligands such as pyrazolates,[6] cyclopentadienes,[7] β-diketonates,[5,8−12] polyethers,[13] and phenolates.[14] However,

*To whom correspondence should be addressed. E-mail: kruhland@syr.edu. Phone: 315-334-1306. Fax: 315-443-4070.

(1) Beno, M. A.; Soderholm, L.; Capone, D. W., II; Hinks, D. G.; Jorgensen, J. D.; Grace, J. D.; Schuller, I. K.; Segre, C. U.; Zhang, K. *Appl. Phys. Lett.* **1987**, *51*, 57–59. Watson, I. M. *Chem. Vap. Deposition* **1997**, *3*, 9–26. Bade, J. P.; Baker, E. A.; Kingon, A. I.; Davis, R. F.; Bachmann, K. J. *J. Vac. Sci. Technol., B: Microelectron. Nanometer Struct.* **1990**, *8*, 327–331. Dickinson, P. H.; Geballe, T. H.; Sanjurjo, A.; Hildenbrand, D.; Craig, G.; Zisk, M.; Collman, J.; Banning, S. A.; Sievers, R. E. *J. Appl. Phys.* **1989**, *66*, 444–447. Zhao, J.; Dahmen, K. H.; Marcy, H. O.; Tonge, L. M.; Marks, T. J.; Wessels, B. W.; Kannewurf, C. R. *Appl. Phys. Lett.* **1988**, *53*, 1750–1752. Yamane, H.; Kurosawa, H.; Hirai, T.; Watanabe, K.; Iwasaki, H.; Kobayashi, N.; Muto, Y. *J. Cryst. Growth* **1989**, *98*, 860–866. Berry, A. D.; Gaskill, D. K.; Holm, R. T.; Cukauskas, E. J.; Kaplan, R.; Henry, R. L. *Appl. Phys. Lett.* **1988**, *52*, 1743–1745.

(2) Kwak, B. S.; Zhang, K.; Boyd, E. P.; Erbil, A.; Wilkens, B. J. *J. Appl. Phys.* **1991**, *69*, 767–772.

(3) Zhang, J. M.; Wessels, B. W.; Richeson, D. S.; Marks, T. J.; DeGroot, D. C.; Kannewurf, C. R. *J. Appl. Phys.* **1991**, *69*, 2743–2745.

(4) Singh, R.; Sinha, S.; Chou, P.; Hsu, N. J.; Radpour, F.; Ullal, H. S.; Nelson, A. J. *J. Appl. Phys.* **1989**, *66*, 6179–6181. Mao, Y.; Zhang, F.; Wong, S. S. *Adv. Mater.* **2006**, *18*, 1895–1899. Bouffard, M.; Jouart, J. P.; Mary, G. *J. Phys. IV.* **1994**, *4*, C4/439–C4/42. Grass, R. N.; Stark, W. J. *Chem. Commun. (Cambridge, U. K.).* **2005**, 1767–1769. Jamison, S. P.; Reeves, R. J. *Phys. Rev. B: Condens. Matter Mater. Phys.* **2003**, *67*, 115110/1–115110/16.

(5) Purdy, A. P.; Berry, A. D.; Holm, R. T.; Fatemi, M.; Gaskill, D. K. *Inorg. Chem.* **1989**, *28*, 2799–2803.

(6) Hitzbleck, J.; Deacon, G. B.; Ruhlandt-Senge, K. *Angew. Chem., Int. Ed.* **2004**, *43*, 5218–5220. Hitzbleck, J.; O'Brien, A. Y.; Forsyth, C. M.; Deacon, G. B.; Ruhlandt-Senge, K. *Chem.—Eur. J.* **2004**, *10*, 3315–3323. Pfeiffer, D.; Heeg, M. J.; Winter, C. H. *Inorg. Chem.* **2000**, *39*, 2377–2384. Hitzbleck, J.; O'Brien, A. Y.; Deacon, G. B.; Ruhlandt-Senge, K. *Inorg. Chem.* **2006**, *45*, 10329–10337.

(7) Hanusa, T. P. *Chem. Rev.* (*Washington, D. C.*) **1993**, *93*, 1023–1036. Hanusa, T. P. *Polyhedron* **1990**, *9*, 1345–1362. Hatanpaeae, T.; Vehkamaeki, M.; Mutikainen, I.; Kansikas, J.; Ritala, M.; Leskelae, M. *Dalton Trans.* **2004**, 1181–1188.

(8) Timmer, K.; Spee, K. I. M. A.; Mackor, A.; Meinema, H. A.; Spek, A. L.; Van der Sluis, P. *Inorg. Chim. Acta* **1991**, *190*, 109–117.

(9) Drake, S. R.; Hursthouse, M. B.; Abdul Malik, K. M.; Miller, S. A. S. *Inorg. Chem.* **1993**, *32*, 4653–4657.

(10) Nash, J. A. P.; Barnes, J. c.; Cole-Hamilton, D. J.; Richards, B. C.; Cook, S. L.; Hitchman, M. L. *Adv. Mater. Opt. Electron.* **1995**, *5*, 1–10.

(11) Bradley, D. C.; Hasan, M.; Hursthouse, M. B.; Motevalli, M.; Khan, O. F. Z.; Pritchard, R. G.; Williams, J. O. *J. Chem. Soc., Chem. Commun.* **1992**, 575–576. Gilliland, D. G.; Hitchman, M. L.; Thompson, S. C.; Cole-Hamilton, D. J. *J. Phys. III.* **1992**, *2*, 1381–1389. Drozdov, A. A.; Troyanov, S. I. *Polyhedron* **1992**, *11*, 2877–2882.

(12) Norman, J. A. T.; Pez, G. P. *J. Chem. Soc., Chem. Commun.* **1991**, 971–972.

(13) Chi, Y.; Ranjan, S.; Chung, P.-W.; Hsieh, H.-Y.; Peng, S.-M.; Lee, G.-H. *Inorg. Chim. Acta* **2002**, *334*, 172–182. Herrmann, W. A.; Huber, N. W.; Priermeier, T. *Angew. Chem.* **1994**, *106*, 102–104. Herrmann, W. A.; Huber, N. W.; Priermeier, T. *Angew. Chem., Int. Ed. Engl.* **1994**, *33*(1), 105–107.

(14) Maudez, W.; Haeussinger, D.; Fromm, K. M. *Z. Anorg. Allg. Chem.* **2006**, *632*, 2295–2298.

 Published on Web 07/09/2010

Table 1. Crystallographic Data for Compounds **1b**, **2b−c**, and **3b−d**

	1b	**1c**	**2b**	**2c**	**2d**	**3b**	**3c**	**3d**
empirical formula	$C_{24}H_{32}O_6F_{18}Ca$	$C_{24}H_{32}O_6F_{18}Sr$	$C_{16}H_{20}O_6F_{18}Ca$	$C_{16}H_{20}O_6F_{18}Sr$	$C_{20}H_{30}O_8F_{18}Ba$	$C_{20}H_{28}O_8F_{18}Ca$	$C_{20}H_{28}O_8F_{18}Sr$	$C_{20}H_{28}O_8F_{18}Ba$
formula weight	798.58	846.12	690.40	737.94	877.78	778.50	826.04	875.76
temperature (K)	96(2)	99(2)	96(2)	97(2)	96(2)	98(2)	101(2)	98(2)
space group	*P*2(1)	*Pna*2(1)	*C*2/*c*	*Pbca*	*P*2(1)/*n*	$P\bar{1}$	*P*2(1)/*n*	*P*2(1)/*n*
a (Å)	9.9635(7)	21.077(2)	29.271(4)	11.424(1)	9.4515(9)	10.087(1)	10.389(1)	10.421(1)
b (Å)	17.022(1)	9.122(1)	10.503(1)	17.264(2)	14.311(1)	16.763(2)	10.649(1)	10.905(1)
c (Å)	10.7552(8)	17.296(2)	17.645(3)	27.885(3)	12.134(1)	18.870(2)	14.140(2)	14.213(2)
α (deg)	90	90	90	90	90	96.385(2)	90	90
β (deg)	116.790(1)	90	101.536(3)	90	90.402(2)	103.236(3)	101.871(2)	103.010(2)
γ (deg)	90	90	90	90	90	93.519(2)	90	90
V (Å^3)	1628.3(2)	3325.3(6)	5314.9(14)	5499.4(11)	1641.2(3)	3074.1(6)	1530.9(3)	1573.8(4)
Z	2	4	8	8	2	4	2	2
crystal size (mm)	0.38 × 0.36 × 0.36	0.30 × 0.22 × 0.20	0.16 × 0.12 × 0.10	0.16 × 0.08 × 0.08	0.22 × 0.12 × 0.05	0.27 × 0.20 × 0.18	0.40 × 0.30 × 0.06	0.50 × 0.50 × 0.30
D_{calc} (Mg/m^3)	1.629	1.690	1.726	1.783	1.776	1.682	1.792	1.848
linear abs. coeff. (mm^{-1})	0.333	1.758	0.393	2.112	1.351	0.355	1.912	1.409
θ range (deg)	2.12−28.36	1.93−28.44	2.36−28.32	2.30−28.38	2.20−28.35	1.55−28.32	2.23−28.30	2.20−28.31
no. indep. reflns.	8039	8297	6592	6865	4071	15204	3795	3912
no. of parameters	453	562	409	409	334	847	300	300
R1, wR2 (all data)	R1 = 0.0595, wR2 = 0.1314	R1 = 0.0852, wR2 = 0.1227	R1 = 0.1164, wR2 = 0.1212	R1 = 0.1185, wR2 = 0.1154	R1 = 0.0587, wR2 = 0.1148	R1 = 0.1319, wR2 = 0.1411	R1 = 0.0291, wR2 = 0.0561	R1 = 0.0191, wR2 = 0.0442
R1, wR2 (> 2*σ*)	R1 = 0.0532, wR2 = 0.1270	R1 = 0.0510, wR2 = 0.1094	R1 = 0.0537, wR2 = 0.0994	R1 = 0.0499, wR2 = 0.0936	R1 = 0.0419, wR2 = 0.1066	R1 = 0.0605, wR2 = 0.1167	R1 = 0.0224, wR2 = 0.0536	R1 = 0.0162, wR2 = 0.0423

alkaline earth metals, specifically barium, form oligomeric compounds resulting in low volatility. As an example, the commercially utilized barium β-diketonate exists as a tetrameric formulation, resulting in relatively high temperature requirements for volatilization. Improvements upon existing successful ligand systems are in high demand.

The perfluoro-*tert*-butoxide (PFTB) ligand has several advantages over *t*-butoxide and other simple alkyl ligands. The enhanced strength of the C−F over the C−H bond (C−H: 411 kJ mol^{-1}; C−F: 485 kJ mol^{-1})[15] leading toward greater thermal stability, multiple non-bonding p-electrons shielding the carbon backbone, and the presence of strong electron withdrawing groups may add beneficial inductive effects to the molecule;[16,17] as demonstrated by the significant increase in pK_a for the alcoholic proton [H(PFTB): 5.4, aqueous; *t*-butanol: 19.2, aqueous].[17] Furthermore, PFTB complexes show relative stability when compared to other partially fluorinated alkoxides.[18] The fluorine saturation safeguards against the frequently observed decomposition pathways of partially fluorinated alkoxides.

This study emphasizes the use of PFTB as a ligand. Unlike other simple fluoroalkoxides, only few studies focus on PFTB. Few fully characterized monometallic PFTB complexes exist, including [Li(PFTB)(thf)$_2$]$_2$,[19] [Li(PFTB)]$_4$,[19] and [Na(PFTB)]$_4$.[20] Likewise, Andersen et al. reported a monometallic beryllium complex characterized by ^{19}F NMR, elemental analysis, and cryoscopic measurements.[21] Co-ligand free calcium, strontium, and barium derivatives were prepared by Purdy et al.,[22,23] although, only ^{19}F NMR, elemental analysis and sublimation studies were reported providing compounds of moderate volatility. The degree of aggregation and structural details remain unknown.

Our efforts lead to the utilization of PFTB, resulting in the isolation of a family of alkaline earth PFTB complexes that contain co-ligands to increase the volatility of the complexes. All complexes are monomeric and contain coordinated co-ligands, following the general formula, [Ae(PFTB)$_2$(d)$_x$]; [**1a**, [Mg(PFTB)$_2$(thf)$_2$]; **1b**, [Ca(PFTB)$_2$(thf)$_4$]; **1c**, [Sr(PFTB)$_2$(thf)$_4$]; **1d**, [Ba(PFTB)$_2$(thf)$_4$]; **2a**, [Mg(PFTB)$_2$(dme)]; **2b**, [Ca(PFTB)$_2$(dme)$_2$]; **2c**, [Sr(PFTB)$_2$(dme)$_2$]; **2d**, [Ba(PFTB)$_2$(dme)$_3$]; **3a**, [Mg(PFTB)$_2$(diglyme)]; **3b**, [Ca(PFTB)$_2$(diglyme)$_2$]; **3c**, [Sr(PFTB)$_2$(diglyme)$_2$]; **3d**, [Ba(PFTB)$_2$(diglyme)$_2$]]. Furthermore, we report several improved synthetic strategies (alkane elimination, direct metalation via ammonia activation, transamination, and co-ligand exchange reactions) to yield the target compounds in a significantly shorter time period in high yield and purity. Analysis utilizing IR and multinuclear NMR spectroscopy, as well as single crystal X-ray diffraction revealed that many of the complexes are monomeric. Thermogravimetric analysis (TGA) of all the compounds demonstrates impressively the effectiveness of co-ligand selection on the volatility of the resulting complexes.

Scheme 1

Method A: Alkane Elimination

$$Mg(Bu)_2 + 2\ H(PFTB) \xrightarrow{THF} [Mg(PFTB)_2(thf)_2] + 2\ H(Bu)$$

Method B: Direct Metallation *via* Ammonia Activation

$$Ae + 2\ H(PFTB) \xrightarrow[NH_3\ (l)]{THF} [Ae(PFTB)_2(thf)_4] + H_2$$

Ae = Ca, Sr, Ba

Method C: Transamination

$$Ae(HMDS)_2(thf)_2 + 2\ H(PFTB) \xrightarrow{THF} [Ae(PFTB)_2(thf)_4] + 2\ H(HMDS)$$

Ae = Ca, Sr, Ba HMDS = hexamethyldisilazane, N(SiMe$_3$)$_2$

As briefly mentioned above, co-ligand free alkaline earth complexes were reported in the literature;[22,23] however, insufficient characterization lead to an incomplete understanding of the aggregation tendencies and therefore an incorrect assessment of the volatility. The reported calcium (**1b**, **2b**, **3b**), strontium (**1c**, **2c**, **3c**), and barium (**1d**, **2d**, **3d**) complexes all contain co-ligands and exhibit a significant increase in their volatilities compared with the previously reported complexes.[22,23]

2. Experimental Section

2.1. General Methods. All compounds were prepared and handled using a glovebox (N_2 atmosphere) and modified Schlenk techniques with a purified Ar atmosphere and special concerns for limiting exposure to water and oxygen. H(PFTB) was obtained commercially and purified by reflux and distillation from calcium hydride, followed by storage in a Schlenk flask at −13 °C. Diglyme was refluxed over calcium hydride and vacuum distilled prior to use. The Ae(HMDS)$_2$(thf)$_2$ (Ae = Ca, Sr, Ba; HMDS = hexamethydisilazide, $^-$[N(Si(CH$_3$)$_3$)$_2$]) starting materials were prepared according to literature methods.[24] All other solvents or co-ligands were collected from a solvent purification system and degassed using three freeze/thaw cycles before use. Anhydrous ammonia was obtained by condensing ammonia gas onto sodium metal using a dry ice-acetone bath.

IR spectra were collected using the Nicolet L200 FTIR spectrometer over the range of 4000 to 400 cm^{-1}. IR samples were prepared using mineral oil mulls sandwiched between KBr plates. ^{1}H, ^{13}C, and ^{19}F NMR spectra were collected using a 300 MHz Bruker Avance spectrometer. Chemical shifts are referenced to residual solvent signals from [D$_6$]benzene (7.16 ppm). Fluorine NMR spectra are referenced externally with trifluoroacetic acid (−76.5 ppm). Elemental analyses were not performed as the described complexes desolvate easily.

2.2. Thermogravimetric Analysis (TGA). The TA Q 500 Instrument was used to perform the analyses. Sample sizes between 5 to 30 mg were loaded onto platinum pans. Purified nitrogen gas was used for all samples with a balance purge rate of 40 mL/min and a sample purge rate of 60 mL/min. The temperature was ramped at 10 °C per minute until a final temperature of 700 °C was reached.

2.3. Crystallographic Data and Refinement Details. Single crystal experiments were carried out using the Bruker AXS SMART CCD system with three-circle goniometer APEX

(15) Huheey, J. E.; Keiter, E. A.; Keiter, R. L. *Inorganic Chemistry: Principles of Structure and Reactivity*; Harper Collins: New York, 1993.
(16) Chambers, R. D. *Fluorine in Organic Chemistry*; Blackwell Publishing Ltd: Boca Raton, FL, 2004.
(17) Willis, C. J. *Coord. Chem. Rev.* **1988**, *88*, 133–202.
(18) Samuels, J. A.; Chiang, W.-C.; Yu, C.-P.; Apen, E.; Smith, D. C.; Baxter, D. V.; Caulton, K. G. *Chem. Mater.* **1994**, *6*, 1684–1692.
(19) Reisinger, A.; Trapp, N.; Krossing, I. *Organometallics.* **2007**, *26*, 2096–2105.
(20) Samuels, J. A.; Folting, K.; Huffman, J. C.; Caulton, K. G. *Chem. Mater.* **1995**, *7*, 929–935.
(21) Andersen, R. A.; Coates, G. E. *J. Chem. Soc., Dalton Trans.* **1975**, 1244–1245.
(22) Purdy, A. P.; George, C. F. *Inorg. Chem.* **1991**, *30*, 1969–1970.
(23) Purdy, A. P.; George, C. F.; Callahan, J. H. *Inorg. Chem.* **1991**, *30*, 2812–2819.
(24) Gillett-Kunnath, M. M.; MacLellan, J. G.; Forsyth, C. M.; Andrews, P. C.; Deacon, G. B.; Ruhlandt-Senge, K. *Chem. Commun.* (*Cambridge, U. K.*) **2008**, 4490–4492.

Scheme 2

$$[Ae(PFTB)_2(thf)_x] \xrightarrow{\text{co-ligand}} [Ae(PFTB)_2(\text{co-ligand})_y] + x\ THF$$

Reagent	x	solvent	Product	co-ligand	y	Yield (%)
1a	2	DME	**2a**	DME	1	29
1a*	2	THF/diglyme	**3a**	diglyme	1	47
1b	4	DME	**2b**	DME	2	44
1b*	4	THF/diglyme	**3b**	diglyme	2	55
1c	4	DME	**2c**	DME	2	82
1c*	4	THF/diglyme	**3c**	diglyme	2	73
1d	4	DME	**2d**	DME	3	95
1d*	4	THF/diglyme	**3d**	diglyme	2	66

* **Reagent from in situ Method C.**

detector, graphite-monochromated Mo Kα radiation (λ = 0.71073 Å), and narrow frame exposures of 0.3° in θ. A hemisphere of data was collected at low temperatures; cell parameters were refined using SMART and integrated using SAINT. The final structures (Table 1) were solved and refined using SHELXS-97 and SHELXL-97.[25] PLATON was used to check the space group assignment of **1b**.[26]

CCDC 775809 (**1b**), 775810 (**1c**), 775811 (**2b**), 775812 (**2c**), 775813 (**2d**), 775814 (**3b**), 775815 (**3c**), and 775816 (**3d**) contains the supplementary crystallographic data for this paper. These data can be obtained free of charge from The Cambridge Crystallographic Data Centre via www.ccdc.cam.ac.uk/data_request/cif.

Many of the crystallographically characterized compounds exhibit positional disorder. In most cases the fluoromethyl groups of the PFTB ligand were disordered, although, in all cases a satisfactory refinement was possible by introducing split positions where the fluorine atoms and the carbon atom of each fluoromethyl were allowed to rotate about the central carbon of the PFTB ligand. Additionally, the co-ligands were disordered but, again introduction of split positions allowed satisfactory refinement.

[*cis*-Ca(PFTB)$_2$(thf)$_4$] (**1b**): THF: 40/60, 42/58;

[*cis*-Sr(PFTB)$_2$(thf)$_4$](**1c**): PFTB: 37/67, 32/68, 27/73, 21/79, 18/82, 11/89, THF: 42/58, 36/64, 37/63;

[*cis*-Ca(PFTB)$_2$(dme)$_2$] (**2b**): PFTB: 28/72, 28/72, 31/69;

[*cis*-Sr(PFTB)$_2$(dme)$_2$] (**2c**): PFTB: 21/79, 23/77, 19/81;

[*trans*-Ba(PFTB)$_2$(dme)$_3$] (**2d**): PFTB: 36/64, 15/85, 39/61, DME: 50/50, 50/50, 50/50;

[*trans*-Sr(PFTB)$_2$(diglyme)$_2$] (**3c**): PFTB: 22/78, 20/80, 18/82;

[*trans*-Ba(PFTB)$_2$(diglyme)$_2$] (**3d**): PFTB: 47/53, 42/58, 49/51.

3. Synthesis

General Procedure. Anhydrous Ammonia. A 3-neck 500 mL round-bottom was fitted with a dry ice condenser and dry ice/acetone bath; ammonia gas was allowed to condense in the flask onto sodium metal, leading to a deep blue solution.

Method A: Alkane Elimination (M = Mg). A 100 mL Schlenk tube was charged with tetrahydrofuran (THF, 10 mL), and H(PFTB) (4 mmol, 0.57 mL). Dibutyl magnesium (2 mmol, 1 M, 2 mL) was slowly added via a syringe, which resulted in a slight temperature increase, but the solution remained clear. The solution was stirred for 1 h at room temperature, then all volatiles were removed by evacuation. A white solid remained, which was redissolved in a minimal amount of THF (1.5 mL) layered with 5 mL of hexane and left to crystallize at room temperature.

Method B: Direct Metalation via Ammonia Activation (M = Ca, Sr, Ba). Anhydrous ammonia, as prepared above, was recondensed into a 2-neck 500 mL round-bottom flask fitted with a dry ice condenser. The flask was charged with alkaline earth metal (10 mmol, Ca; 0.40 g, Sr; 0.87 g, Ba; 1.37 g) and H(PFTB) (20 mmol, 2.8 mL) in THF (10−20 mL) and cooled utilizing a dry ice-acetone bath. When ammonia condensed into the flask, the solution turned a blue color. The dry ice-acetone bath was removed, and the solution was allowed to reflux forming a blue solution that became colorless within 1 h. Excess ammonia was allowed to evaporate overnight. All remaining volatiles were removed by evacuation, leaving a white powdery residue, which was redissolved in 20 mL of THF, filtered through a Celite padded frit, concentrated, and placed into a −23 °C freezer to crystallize. Crystallization occurred within 2 days, yielding in all cases colorless crystals.

Method C: Transamination (M = Ca, Sr, Ba). At room temperature H(PFTB) (4 mmol, 0.56 mL) was slowly added by syringe into a 100 mL Schlenk tube charged with Ae(HMDS)$_2$(thf)$_2$ (Ae = 2 mmol, 1.01 g: Ca; 2 mmol, 1.10 g: Sr; 2 mmol, 1.20 g: Ba), dissolved in 5 mL of THF. The solution was stirred for 1 h, resulting in a pale yellow color for all compounds. All volatiles were removed by evacuation leaving a yellow-cream colored precipitate. The residue was redissolved in a small amount of THF (<5 mL); filtered over a Celite padded frit, concentrated, layered with 10 mL of hexane and placed into a 5 °C freezer to crystallize. Crystallization typically occurred within 2 days. Slight variations in procedure are listed individually below.

[Mg(PFTB)$_2$(thf)$_2$] (1a). Method A: yield 1.09 g (86%). Colorless plates; Mp (sealed tube/N_2): 83−84 °C (wetting), 117−123 °C (melt), 280−290 °C (dec); ^{1}H NMR (300 MHz, C_6D_6): δ = 1.1 (m, 2H, $-CH_2-$), 3.4 (m, 2H, $-OCH_2-$); ^{13}C NMR (300 MHz, C_6D_6): δ = 25.0 (s, $-CH_2-$), 70.0 (s, $-OCH_2-$); ^{19}F NMR (300 MHz, C_6D_6): δ = −76.8 (s, $-CF_3$); IR (Nujol mull, cm^{-1}): 2924(s), 2852(s), 2394(w), 1461(m), 1377(m), 1248(w), 1170(w), 1050(w), 970(w), 825(w), 725(w).

[*cis*-Ca(PFTB)$_2$(thf)$_4$] (1b). Method B: 7.98 g (100%); multiple crystal crops were grown and collected.

Method C: 4.39 g (92%); The reaction was carried out as described above, except that the scale was increased to 6 mmol.

Colorless block; Mp (sealed tube/N_2): 109−110 °C, 375 °C (dec); ^{1}H NMR (300 MHz, C_6D_6): δ = 1.4 (m, 2H, $-CH_2-$), 3.6 (m, 2H, $-OCH_2-$); ^{13}C NMR (300 MHz,

(25) Sheldrick, G. M. Madison, WI (USA). Siemens. 1997.
(26) Speck, A. L. *PLATON, A Multipurpose Crystallographic Tool*; Utrecht University: Utrecht, The Netherlands, 2000.

C_6D_6): δ = 25.4 (s, $-CH_2-$), 68.7 (s, $-OCH_2-$); ^{19}F NMR (300 MHz, C_6D_6): δ = −75.9 (s, $-CF_3$); IR (Nujol mull, cm^{-1}): 2924(s), 2851(s), 1461(s), 1376(s), 1299(m), 1261(m), 1217(m), 1141(w), 1040(w), 959(w), 883(w), 723(w), 669(w), 533(w).

[*cis*-Sr(PFTB)$_2$(thf)$_4$] (1c). Method B: 8.46 g (100%); multiple crystal crops were grown and collected.

Method C: 3.50 g (69%); The reaction was carried out as described above except that the scale was increased to 6 mmol.

Colorless plates; Mp (sealed tube/N_2): 197−210 °C (wetting), 350 °C (dec); ^1H NMR (300 MHz, C_6D_6): δ = 1.3 (m, 2H, $-CH_2-$), 3.5 (m, 2H, $-OCH_2-$); ^{13}C NMR (300 MHz, C_6D_6): δ = 25.7 (s, $-CH_2-$), 68.1 (s, $-OCH_2-$); ^{19}F NMR (300 MHz, C_6D_6): δ = −75.7 (s, $-CF_3$); IR (Nujol mull, cm^{-1}): 2923(s), 2854(s), 1461(s), 1376(s), 1302(m), 1272(m), 1208(w), 1191(w), 1029(w), 965(w), 891(w), 825(w), 723(w), 554(w), 532(w).

[Ba(PFTB)$_2$(thf)$_4$] (1d). Method B: 8.82 g (99%).

Colorless needles; Mp (sealed tube/N_2): 350 °C (dec); ^1H NMR (300 MHz, C_6D_6): δ = 1.4(m, 2H, $-CH_2-$), 3.5(m, 2H, $-OCH_2-$); ^{13}C NMR (300 MHz, C_6D_6): δ = 25.9 (s, $-CH_2-$), 67.9 (s, $-OCH_2-$; ^{19}F NMR (300 MHz, C_6D_6): δ = −76.42 (s, $-CF_3$); IR (Nujol mull, cm^{-1}): 2913(s), 1461(s), 1376(s), 1304(m), 1263(m), 1184(m), 1035(w), 956(m), 877(w), 825(w), 724(w), 532(w).

[Mg(PFTB)$_2$(dme)] (2a). Colorless block; 0.07 g (29%); Mp (sealed tube/N_2): 122−125 °C (melt); ^1H NMR (300 MHz, C_6D_6): δ = 2.9 (s, 4H, $-OCH_2-$), 3.0 (s, 6H, $-CH_3$); ^{19}F NMR (300 MHz, C_6D_6): δ = −75.3 (s, $-CF_3$); IR (Nujol mull, cm^{-1}): 2919(s), 1461(s), 1376(s), 1257(m), 1203(m), 1145(w), 1113(w), 1069(w), 1029(w), 955(m), 876(w), 723(m).

[*cis*-Ca(PFTB)$_2$(dme)$_2$] (2b). In a 100 mL Schlenk tube 0.47 g of **1b** was dissolved in 15 mL of 1,2-dimethoxyethane (DME). The solution was stirred for 1 h filtered through a Celite padded frit and concentrated. This solution was then layered with 5 mL of hexane and left to crystallize at room temperature; colorless blocks formed within 2 days. 0.18 g (44%)

Colorless plates; Mp (sealed tube/N_2): 162−167 °C (melt), 280 °C (dec).^1H NMR (300 MHz, C_6D_6): δ = 3.06 (s, 6H, $-CH_3$), 2.8 (s, 4H, $-OCH_2-$); ^{13}C NMR (300 MHz, C_6D_6): δ = 59.5, (s, DME), 70.4 (s, DME); ^{19}F NMR (300 MHz, C_6D_6): δ = −76.3 (s, $-CF_3$); IR (Nujol mull, cm^{-1}): 1297(w), 1264(w), 1201(w), 1147(w), 1114(w), 1069(w), 957(w).

[*cis*-Sr(PFTB)$_2$(dme)$_2$] (2c). In a 100 mL Schlenk tube 0.70 g of **1c** was dissolved in 15 mL of DME. The solution was stirred for 1 h filtered through a Celite padded frit and concentrated. This solution was placed into a −23 °C freezer to crystallize; colorless blocks formed within 2 days. 0.50 g (82%)

Colorless plates; Mp (sealed tube/N_2): 117−122 °C (melt), 300 °C (dec); ^1H NMR (300 MHz, C_6D_6): δ = 3.0 (s, 6H, $-CH_3$), 2.8 (s, 4H, $-OCH_2-$); ^{13}C NMR (300 MHz, C_6D_6): δ = 59.1 (s, DME), 70.9 (s, DME); ^{19}F NMR (300 MHz, C_6D_6): δ = −76.3 (s, $-CF_3$); IR (Nujol mull, cm^{-1}): 1297(m), 1262(m), 1206(m), 1116(w), 1069(m), 1028(w), 862(w).

[*trans*-Ba(PFTB)$_2$(dme)$_3$] (2d). A 100 mL Schlenk tube was charged with 0.43 g of **1d**. The solid was dissolved in 10 mL of DME, stirred for 2 h, whereupon the solvent volume was reduced and the solution was placed into a −23 °C to crystallize. 0.36 g (95%) yield.

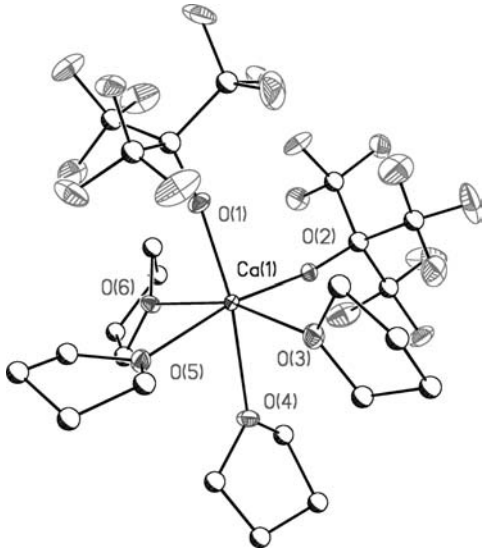

Figure 1. Illustration of [Ca(PFTB)$_2$(thf)$_4$] (**1b**) where the ligands adopt a *cis* conformation. [Sr(PFTB)$_2$(thf)$_4$] (**1c**) is isostructural to **1b**. All non carbon atoms shown at 30% probability and hydrogen atoms have been removed for clarity.

Colorless block; Mp (sealed tube/N_2): 64−67 °C (melt).^1H NMR (300 MHz, C_6D_6): δ = 3.0 (s, 6H, $-CH_3$), 3.1 (s, 4H, $-OCH_2-$); ^{13}C NMR (300 MHz, C_6D_6): δ = 58.7 (s, DME), 71.6 (s, DME); ^{19}F NMR (300 MHz, C_6D_6): δ = −75.7 (s, $-CF_3$); IR (Nujol mull, cm^{-1}): 2912(s), 1461(s), 1376(s), 1302(m), 1262(m), 1205(w), 1070(w), 1032(w), 958(w), 856(w), 722(w).

[Mg(PFTB)$_2$(diglyme)] (3a). Colorless block; 0.28 g (47%); Mp (sealed tube/N_2): 196−198 °C (melt); ^1H NMR (300 MHz, C_6D_6): δ = 3.0 (s, 6H, $-CH_3$), 3.3 (m, 4H, $-OCH_2-$), 3.5. (m, 4H, $-OCH_2-$); ^{19}F NMR (300 MHz, C_6D_6): δ = −74.5 (s, $-CF_3$); FTIR (Nujol mull, cm^{-1}): 1296(w), 1259(w), 1219(w), 1160(w), 1091(w), 1063(w).

[*trans*-Ca(PFTB)$_2$(diglyme)$_2$] (3b). Method C: 0.88 g (55%) yield. Preparation followed Method C, except that after the initial hour of stirring, diglyme (4 mmol, 0.57 mL) was added followed by an additional hour of stirring. All volatiles were removed under reduced pressure leaving a cream colored, powdery residue. A minimal amount of THF (1 mL) redissolved the solid, and the solution was layered with 10 mL of hexane, and crystallized in a 5 °C freezer after 24 h.

Colorless needles; Mp (sealed tube/N_2): 78−79 °C (melt); ^1H NMR (300 MHz, C_6D_6): δ = 3.07 (s, 6H, $-CH_3$), 3.14 (m, 4H, $-OCH_2-$), 3.34 (m, 4H, $-OCH_2-$); ^{13}C NMR (300 MHz, C_6D_6): δ = 59.2 (s, $-OCH_3$), 68.7 (s, $-OCH_2$), 71.2 (s, $-OCH_2$), none observed for PFTB; ^{19}F NMR (300 MHz, C_6D_6): δ = −75.6 (s, $-CF_3$); IR (Nujol mull, cm^{-1}): 1300(m), 1258(m), 1230(m), 1200(m), 1140(w), 1096(w), 1067(w), 955(m), 868(w), 723(s), 532(w).

[*trans*-Sr(PFTB)$_2$(diglyme)$_2$] (3c). Method C: 1.23 g (73%) yield: Preparation followed Method C, except that after the initial hour of stirring, diglyme (4 mmol, 0.57 mL) was added followed by an additional hour of stirring. All volatiles were removed under reduced pressure leaving a cream colored, powdery residue. A minimal amount

Table 2. Select Bond Distances and Angles for **1b**−**c**

	distance (Å)			angle (deg)	
	1b (M = Ca)	**1c** (M = Sr)		**1b** (M = Ca)	**1c** (M = Sr)
M−O(1)	2.183(2)	2.338(4)	O(1)−M−O(2)	103.93(9)	112.96(15)
M−O(2)	2.205(2)	2.328(4)	O(1)−M−O(3)	95.05(9)	92.9(6)
M−O(3)	2.404(2)	2.48(2)	O(1)−M−O(4)	167.36(9)	154.7(6)
M−O(4)	2.428(2)	2.62(3)	O(1)−M−O(5)	87.29(9)	82.67(14)
M−O(5)	2.434(2)	2.584(3)	O(1)−M−O(6)	97.56(8)	90.44(13)
M−O(6)	2.416(2)	2.571(3)			

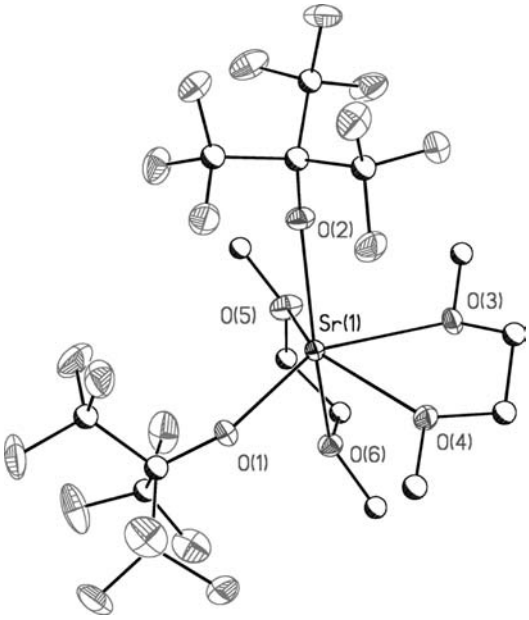

Figure 2. Depiction of the structure of $[Sr(PFTB)_2(dme)_2]$ (**2c**). $[Ca(PFTB)_2(dme)_2]$ (**2b**) is isostructural. All non-carbon atoms are shown at 30% probability, with the hydrogen atoms removed for clarity.

of THF (1 mL) redissolved the solid, and the solution was layered with 10 mL of hexane, and crystallized in a 5 °C freezer after 24 h.

Colorless blocks; Mp (sealed tube/N_2): 152−153 °C (melt); ^{1}H NMR (300 MHz, C_6D_6): δ = 3.08 (m, 4H, $-OCH_3$), 3.12 (s, 6H, $-CH_3$), 3.26 (m, 4H, $-OCH_2-$); ^{13}C NMR (300 MHz, C_6D_6): δ = 59.1 (s, $-CH_3$), 68.9 (s, $-OCH_2$), 71.2 (s, $-OCH_2$), none observed for PFTB; ^{19}F NMR (300 MHz, C_6D_6): δ = −75.9 (s, $-CF_3$); IR (Nujol mull, cm^{-1}): 1254(m), 1208(w), 1136(m), 1103(w), 1077(w), 953(m), 802(m), 722(s).

[*trans*-Ba(PFTB)$_2$(diglyme)$_2$] (3d). Method C: 1.15 g (66%) yield; Preparation followed Method C, except that after the initial hour of stirring, diglyme (4 mmol, 0.57 mL) was added followed by an additional hour of stirring. All volatiles were removed under reduced pressure leaving a cream colored, powdery residue. The cream colored solid was redissolved in THF filter, then placed into a 5 °C where in crystallized within 2 days.

Colorless plates; Mp (sealed tube/N_2): 210 °C (melt); ^{1}H NMR (300 MHz, C_6D_6): δ = 3.04 (m, 4H, $-OCH_3$), 3.13 (s, 6H, $-CH_3$), 3.16 (m, 4H, $-OCH_2-$); ^{13}C NMR (300 MHz, C_6D_6): δ = 58.8(s, $-CH_3$), 69.0 (s, $-OCH_2-$), 71.6 (s, $-OCH_2-$), none observed for PFTB; ^{19}F NMR (300 MHz, C_6D_6): δ = −76.0 (s, $-CF_3$); IR (Nujol mull, cm^{-1}): 1304(m), 1261(m), 1177(m), 1021(w), 955(s), 724(s).

4. Results

4.1. Synthetic Methodology. The target compounds were prepared conveniently by a variety of synthetic procedures in moderate to excellent yields and high purity. This presents a significant improvement over previously reported methods that relied on refluxing the metal and ligand yielding the co-ligand free alkaline earth PFTB complexes. Disadvantages of the prior route include reaction temperatures (90−130 °C) significantly higher than the boiling point of the H(PFTB) ligand (35 °C) for an extended period of time (4−14 days).[23,27] While the published yields were good for strontium (100%) and barium (84%), only 21% conversion was achieved for calcium.[23] We here report on alternative synthetic methodologies that afford all three metal derivatives in good yield and purities; utilizing less strenuous reaction conditions. Further, the improved routes allow the incorporation of co-ligands that, as shown below, have a significant impact on the properties of the compounds.

Three synthetic routes (Methods A−C, Scheme 1) were explored for the preparation of the target complexes, all of which yielded the desired products in moderate to excellent yield with high purity; although not every method is applicable for all the alkaline earth metals. For example, alkane elimination provides outstanding results for the magnesium species, but the challenging preparation and handling of the heavier alkaline earth metal precursors makes this route less attractive, especially in light of potential commercialization. On the other hand, ammonia activation of the metals is amenable only to the heavier metals, as magnesium does not dissolve in anhydrous liquid ammonia. Transamination is applicable for all four metals, but for magnesium it does not offer advantages over the commercially available dibutyl magnesium precursor.

Alkane eliminations were performed in THF solutions of H(PFTB) where the commercially available dibutyl magnesium reagent was added slowly to yield the magnesium complexes. Typical yields for this reaction were excellent and reaction times were very short (only 1 h). The DME and diglyme donor complexes were obtained by co-ligand exchange reactions. Dissolution of **1a** in either a solution of DME for **2a** (29%) or a THF/diglyme solution yielded **3a** (47%, see Scheme 2). Attempts to isolate the DME adduct, **2a**, via THF solutions failed; however, the diglyme adduct, **3a**, could be isolated via THF/diglyme solutions, likely the result of the chelate effect.

The heavier metal derivatives can be prepared by direct metalation via ammonia activation (Method B) and

(27) Purdy, A. U.S. Patent No. 4,982,019, 1991.

Table 3. Select Bond Lengths and Angles for **2b**−**d**

bond lengths (Å)			bond angles (deg)		
	2b (M = Ca)	**2c** (M = Sr)		**2b** (M = Ca)	**2c** (M = Sr)
M−O(1)	2.168(2)	2.343(3)	O(1)−M−O(2)	112.36(8)	115.5(1)
M−O(2)	2.196(2)	2.331(3)	O(1)−M−O(3)	154.45(8)	148.4(1)
M−O(3)	2.419(2)	2.603(2)	O(1)−M−O(4)	87.79(7)	86.99(9)
M−O(4)	2.418(2)	2.561(3)	O(1)−M−O(5)	104.39(8)	119.7(1)
M−O(5)	2.413(2)	2.554(3)	O(1)−M−O(6)	89.42(8)	90.80(9)
M−O(6)	2.480(2)	2.596(3)			
			O(3)−M−O(4)	67.30(7)	62.93(9)
			O(5)−M−O(6)	66.81(8)	63.76(9)
			O(3)−M−O(5)	94.62(7)	83.6(1)
			O(3)−M−O(6)	82.46(7)	80.56(9)

bond lengths (Å)		bond angles (deg)	
	2d[a]		
Ba(1)−O(1)	2.544(3)	O(1)#1−Ba(1)−O(1)	180.0
Ba(1)−O(2)	2.87(2)	O(1)−Ba(1)−O(2)#1	103.9(5)
Ba(1)−O(3)	2.85(2)	O(1)−Ba(1)−O(3)#1	79.9(3)
Ba(1)−O(4)	2.90(2)	O(1)−Ba(1)−O(4)	98.2(4)
Ba(1)−O(5)	2.84(2)	O(1)−Ba(1)−O(5)	82.9(5)
Ba(1)−O(6)	2.84(2)	O(1)−Ba(1)−O(6)#1	96.7(5)
Ba(1)−O(7)	2.83(2)	O(1)−Ba(1)−O(7)	78.1(4)
		O(2)#1−Ba(1)−O(3)#1	53.9(4)
		O(4)−Ba(1)−O(5)	56.7(5)
		O(6)−Ba(1)−O(7)#1	56.6(5)
		O(2)−Ba(1)−O(5)#1	72.1(4)
		O(3)#1−Ba(1)−O(6)#1	68.1(5)

[a] Symmetry transformations used to generate equivalent atoms. **2d**: #1 $-x+1, -y+1, -z+1$.

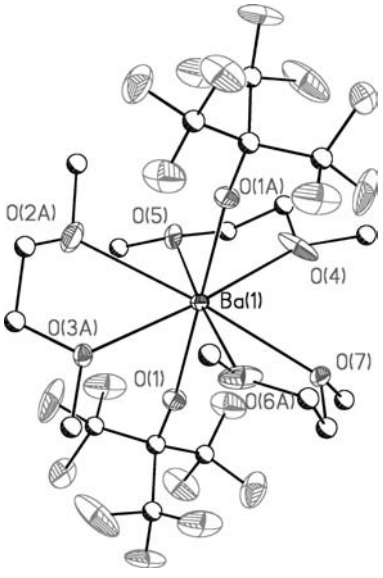

Figure 3. Illustration of $[Ba(PFTB)_2(dme)_3]$ (**2d**). Thermal ellipsoids shown at 30% probability, carbon atoms shown as spheres, and hydrogen atoms removed for clarity.

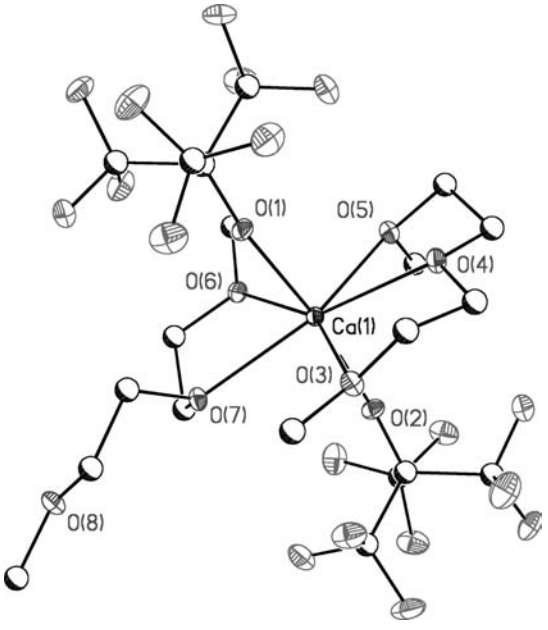

Figure 4. Representation of $[Ca(PFTB)_2(diglyme)_2]$ (**3b**) with all non carbon atoms shown at 30% probability, carbon atoms shown as spheres and all hydrogen atoms not shown for clarity.

transamination (Method C) methodologies. Both afforded the same complexes in significantly shorter reaction times than previously reported.[22,23] However, methods B and C differed in their respective yields, reaction time, and simplicity. Method B (direct metalation in liquid ammonia) gave excellent yields for the THF adduct alkaline earth complexes (**1b**, Ca, 100%; **1c**, Sr, 100%; **1d**, Ba, 99%) with reactions that where complete within an hour. Analogously to the magnesium complexes, a co-ligand exchange reaction with either **1b**−**d** yielded the corresponding co-ligand alkaline earth PFTB complex (see Scheme 2). Method C (transamination) yielded the desired complexes in moderate to good yield (**1b**, 92%; **1c**, 69%; **3b**, 55%; **3c**, 73%; **3d**, 66%) which were complete within a few hours of combining the reagents. The high solubility of the complexes in THF likely decreased the

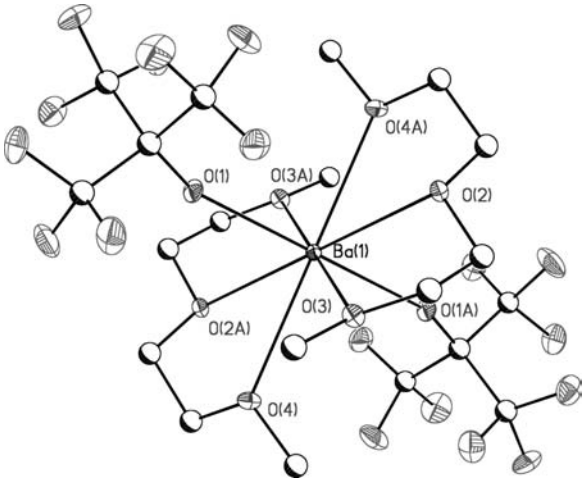

Figure 5. Illustration of $[Ba(PFTB)_2(diglyme)_2]$ (**3d**). $[Sr(PFTB)_2(diglyme)_2]$ (**3c**) is isostructural. All non-carbon atoms shown as ellipsoids with 30% probability, carbon atoms shown as spheres, and all hydrogen atoms removed for clarity.

isolated yield percents; although the products were crystalline and of high purity. Unlike Method B, the diglyme (**3b**−**d**) co-ligand adducts where prepared in situ for the transaminations reactions; allowing fewer synthetic steps. Disadvantages for Method C include the difficult preparation of $Ae(HMDS)_2(thf)_2$; although, more facile methodologies have been recently reported.[24] Analogously to the magnesium species, the DME compounds (**2b**−**d**) were prepared via a co-ligand exchange method (see Scheme 2) from the THF coordinated species.

The target compounds are sensitive to desolvation as exposure to slightly reduced pressure results in the loss of the coordinated co-ligands; making elemental analysis not applicable in determining the correct composition of the isolated complexes. As such the formulas for the described compounds are based on the crystallographic data where available (**1b**−**c**, **2b**−**d**, **3b**−**d**) and further supported by spectroscopic data (IR, multinuclear NMR). The formulas for the non-crystallographically characterized compounds (**1**−**3a**, **1d**) are based on spectroscopic information (IR, multinuclear NMR) and gravimetric analysis. Unfortunately, NMR spectroscopy cannot be utilized to determine exact ligand to co-ligand ratios; these were determined by gravimetric analysis. However, the presence of the co-ligands for **1**−**3a** and **1d** were confirmed by ^{1}H NMR and further supported by ^{13}C NMR. All the samples gave a singlet in the ^{19}F NMR confirming the presence of PFTB.

All reported complexes are non-pyrophoric in nature and can be safely handled in open air. However, prolonged exposure of the complexes to the atmosphere leads to hydration of the complexes.

4.2. Structural Comparisons. A few of the compounds reported **1**−**3a** and **1d** did not afford X-ray quality crystals. Structural information is available for **1b**−**c**, **2b**−**d**, and **3b**−**d**; these complexes are all monomeric and display two general structural motifs with the ligands either in the *cis* or in the *trans* positions. These conformations are coordination number and co-ligand dependent, with the THF adduct adopting only the *cis* conformation, while the DME adducts display both *cis* and *trans*, and the diglyme compounds exhibit exclusively *trans* orientations.

In general the complexes display octahedral or pseudo-octahedral (i.e., pentagonal or hexagonal bipyramidal) geometries with coordination numbers between six and eight. Slight deviations from ideality are noticed in the bond angles; however, the M−O distances are all uniform [Ca−O(PFTB), 2.20(2) Å (av); Ca−O(co-ligand), 2.46(4) Å (av); Sr−O(PFTB), 2.35(2) Å (av); Sr−O(co-ligand), 2.62(9) Å (av); Ba−O(PFTB), 2.539(7) Å (av); Ba−O(co-ligand), 2.86(2) Å (av)]; furthermore, the increase in bond distance smoothly increases with the larger ionic radii [ΔCa→Sr−O(PFTB) = 0.15 Å; ΔCa→Sr (r_{ionic}) = 0.18 Å; Δ*S*r→Ba−O(PFTB) = 0.19 Å; Δ*S*r→Ba (r_{ionic}) = 0.17 Å]. However, the coordination number of the complexes does significantly affect the contact distance of the co-ligand; these differences will be discussed individually, although as expected, the metals co-ligand distance increases with increasing coordination number.

4.2.1. THF Adducted Compounds. The calcium and strontium compounds, $[Ae(PFTB)_2(thf)_4]$ (Ae = Ca, **1b**; Ae = Sr, **1c**) are isostructural to one another (see Figure 1). Both exhibit a distorted octahedral geometry where the *cis* angle between the PFTB ligands are more obtuse [**1b**, 103.93(9)°; **1c**, 112.96(15)°] than the ideal 90°; a result of the steric bulk of the PFTB ligand and from intramolecular F−F repulsions. The M−O bonds agree well with the other complexes in this report [**1b**: Ca−O(PFTB), 2.183(2)−2.205(2) Å; Ca−O(THF), 2.42(2) Å (av); **1c**: Sr−O(PFTB), 2.328(4)−2.338(4) Å; Sr−O(THF), 2.56(6) Å (av); Table 2]. The preference for the *cis* conformation in the THF adducts is unclear, no short contacts between M−F were observed, although polarization of the molecule may explain this conformation.

4.2.2. DME Adducted Complexes. Compounds $[Ae(PFTB)_2(dme)_2]$ (Ae = Ca, **2b**; Ae = Sr, **2c**) are similar to $[Ae(PFTB)_2(thf)_4]$ (Ae = Ca, **1b**; Ae = Sr, **1c**); both form distorted octahedra with the ligands in *cis* conformations (see Figure 2). The similar coordination environments and bond angles result in M−O distances that are similar [**2b**: Ca−O(PFTB), 2.168(2)−2.196(2) Å; Ca−O(DME), 2.43(2) Å (av); **2c**: Sr−O(PFTB), 2.331(3)−2.342(3) Å; Sr−O(DME), 2.58(2) Å (av); Table 3]; here the difference in bond lengths approximate the difference in ionic radii of the metals [ΔM−O(PFTB) = 0.14−0.16 Å; $\Delta M(r_{ionic})$ = 0.18 Å].[28] The slightly larger *cis* angle compared to that of the THF-adducts [**2b**, 112.36(8)°; **2c**, 115.5(1)°] occurs as a result of the smaller steric demands of the bidentate DME. An additional consequence of the smaller co-ligand size is that both **2b**−**c** have a weak, long distance M−F contact [**2b**, 3.033(6) Å; **2c**, 3.24(2) Å]. While these interactions are less than the sum of the Van der Waals radius of fluorine and the metal [Ca−F, 3.9 Å; Sr−F, 4.05 Å],[29] they are not short enough to be considered a significant secondary M−F interaction. Our recent work with the PFTB indicates that M−F interactions may be quantified by using a bond-valence sums analysis, leading to interaction distances that are

(28) Shannon, R. D. *Acta Crystallogr., Sect. A* **1976**, *A32*, 751–767.
(29) Batsanov, S. S. *Inorganic Materials* (*Translation of Neorganicheskie Materialy*) **2001**, *37*, 871–885.

Table 4. Select Bond Distances and Angles for **3b**−**d**

distance (Å)			angle (deg)		
	3b			**3b**	
	molecule A	molecule B		molecule A	molecule B
Ca−O(1)	2.212(2)	2.214(2)	O(1)−Ca(1)−O(2)	172.51(9)	174.74(9)
Ca−O(2)	2.205(2)	2.214(2)	O(1)−Ca(1)−O(3)	86.44(9)	85.19(8)
Ca−O(3)	2.554(2)	2.500(2)	O(1)−Ca(1)−O(4)	88.20(8)	87.65(8)
Ca−O(4)	2.469(2)	2.471(2)	O(1)−Ca(1)−O(5)	102.29(9)	101.55(9)
Ca−O(5)	2.502(2)	2.483(2)	O(1)−Ca(1)−O(6)	90.34(8)	87.00(8)
Ca−O(6)	2.511(2)	2.512(2)	O(1)−Ca(1)−O(7)	86.53(8)	93.22(8)
Ca−O(7)	2.467(2)	2.446(2)			
			O(3)−Ca(1)−O(4)	65.39(8)	65.25(8)
			O(4)−Ca(1)−O(5)	66.47(8)	66.15(8)
			O(6)−Ca(1)−O(7)	68.28(8)	68.27(8)
			O(5)−Ca(1)−O(6)	73.13(8)	75.31(8)
			O(3)−Ca(1)−O(7)	87.87(8)	87.50(8)
distance (Å)			angle (deg)[a]		
	3c (M = Sr)	**3d** (M = Ba)		**3c** (M = Sr)	**3d** (M = Ba)
M−O(1)	2.389(1)	2.5335(9)	O(1)−M−O(1)#1	180.0	180.0
M−O(2)	2.699(1)	2.8622(9)	O(1)−M−O(2)	102.80(3)	104.14(3)
M−O(3)	2.731(1)	2.8435(9)	O(1)−M−O(3)	86.30(3)	89.28(3)
M−O(4)	2.773(1)	2.8835(9)	O(1)−M−O(4)#1	88.18(3)	90.32(3)
			O(2)−M−O(3)	58.99(3)	57.33(3)
			O(2)−M−O(4)#1	59.11(3)	57.58(3)
			O(3)−M−O(4)	65.43(3)	67.52(3)

[a] Symmetry transformations used to generate equivalent atoms. **3c**−**d**: #1 $-x+2$, $-y+2$, $-z$.

Table 5. Critical Thermal Features Belonging to the Alkaline Earth Perfluoro-*t*-butoxide Complexes at Ambient Pressure

compound	T^a (°C)	$T_0{}^b$ (°C)	wt %[c]	wt % (AeF_2)[d]	wt % (AeO)[e]
$[Mg(PFTB)_2(thf)_2]$ (**1a**)	25[g]	350	8.3−12	9.7	6.3
$[Mg(PFTB)_2(dme)]$ (**2a**)	80[f]	300	0.9−1.3	10.6	6.9
$[Mg(PFTB)_2(diglyme)]$ (**3a**)	150	224	1.3−1.7	9.9	6.4
$[Ca(PFTB)_2(thf)_4]$ (**1b**)	88[f]	350	1.6−1.7	9.7	7.0
$[Ca(PFTB)_2(dme)_2]$ (**2b**)	120[f]	250	1.0−2.5	11.8	8.5
$[Ca(PFTB)_2(diglyme)_2]$ (**3b**)	175[f]	400	3.3−6.6	10.0	7.2
$[Sr(PFTB)_2(thf)_4]$ (**1c**)	133	287	0.7−1.1	14.8	12.2
$[Sr(PFTB)_2(dme)_2]$ (**2c**)	179	282	0.2−0.4	17.8	14.6
$[Sr(PFTB)_2(diglyme)_2]$ (**3c**)	175	290	1.4−4.4	15.2	12.5
$[Ba(PFTB)_2(thf)_4]$ (**1d**)	220	368	2.4−8.0	19.6	17.1
$[Ba(PFTB)_2(dme)_3]$ (**2d**)	240	370	7.5−8.0	19.9	17.5
$[Ba(PFTB)_2(diglyme)_2]$ (**3d**)	210	370	5.0−17	20.0	17.5

[a] Onset of complex sublimation (the largest weight percent decrease). [b] Final plateau of TGA profile. [c] Weight percent at T_0. [d] Calculated weight percent for complete conversion to the alkaline earth fluoride. [e] Calculated weight percent for complete conversion to the alkaline earth oxide. [f] Indicates the beginning of the weight loss. [g] Indicates that weight percent change occurred immediately.

Table 6. Representative TGA and Sublimation Data for Alkaline Earth MOCVD Precursors

	TGA				
compound	T^a (°C)	$T_0{}^b$ (°C)	wt %	SP/P[c]	ref.
$[Ca(PFTB)_2]_x$				140/$<10^{-5}$	23
$[Sr(PFTB)_2]_x$				230/$<10^{-5}$	23
$[Ba(PFTB)_2]_x$				280/$<10^{-5}$	23
$Ba(TMHD)_2$(tetraglyme)	320	410	6		10
$Ca(HFA)_2$(triglyme)				$100/2\times10^{-2}$	8
$Sr(HFA)_2$(tetraglyme)				$115/10^{-2}$	8
$Ba(HFA)_2$(hexaglyme)				$145/2\times10^{-2}$	8
$Ba(HFA)_2$(tetraglyme)	125[10]	310[10]	∼5	$120/10^{-3}$	9, 10
$Ba(TDFND)_2$(tetraglyme)	160	305	1		10
$Ba(HFA)_2$(18-crown-6)				$150-200/10^{-3}$	12
$Ba(TMHD)_2(diglyme)_2$	240	402	6		9

[a] Sublimation onset temperature. [b] Sublimation complete temperature. [c] Sublimation point in degrees Celsius at a specific pressure in Torr; TMHD = 2,2,6,6-tetramethly-3,5-heptadione; HFA = hexafluoroacetylacetonate; TDFND = 1,1,1,2,2,3,3,7,7,8,8,9,9,9-tetradecafluorononane-4,5-dione.

significantly shorter;[30] this view is further supported by the literature.[31]

In contrast to the calcium and strontium complexes, the barium species (**2d**) displays a *trans* ligand conformation. A noticeable difference between the Ca/Sr and Ba compounds is the coordination number; **2b**−**c** are hexacoordinated in a distorted octahedral geometry whereas **2d** is eight coordinate, displaying a distorted hexagonal bipyramidal geometry (Figure 3). The three DME coligands occupy a tilted equatorial plane deviating as much as 13.9°, resulting in a tilted belt of coordinated DME co-ligands around the Ba metal center. The Ba−O distances in **2d** [Ba−O(PFTB), 2.544(3) Å; Ba−O(DME), 2.86(3) Å (av)] compare favorably with the average Ba−O(PFTB) bond lengths given above, as well as to Ba−O distances of other simple fluoroalkoxides. For example $Ba_5(\mu_5\text{−}OH)[\mu_3\text{-}OCH(CF_3)_2]_4[\mu_2\text{-}OCH(CF_3)_2]_4[OCH(CF_3)_2](THF)_4(H_2O)\cdot THF$ displays Ba−O bonds between 2.53(3)−2.86(3) Å,[32] and the related $BaAg(PFTB)_3(thf)_4$, has a terminal Ba−O distance of 2.448(12) Å.[33] Not surprisingly and in contrast to **2b**−**c**, the increase in coordinative saturation through additional DME coordination and

(30) Buchanan, W. D.; Ruhlandt-Senge, K., manuscript in preparation.
(31) Plenio, H. *Chem. Rev.* (*Washington, D. C.*) **1997**, *97*, 3363–3384.
(32) Vincent, H.; Labrize, F.; Hubert-Pfalzgraf, L. G. *Polyhedron* **1994**, *13*, 3323–3327.
(33) Purdy, A. P.; George, C. F. *ACS Symp. Ser.* **1994**, *555*, 405–420.

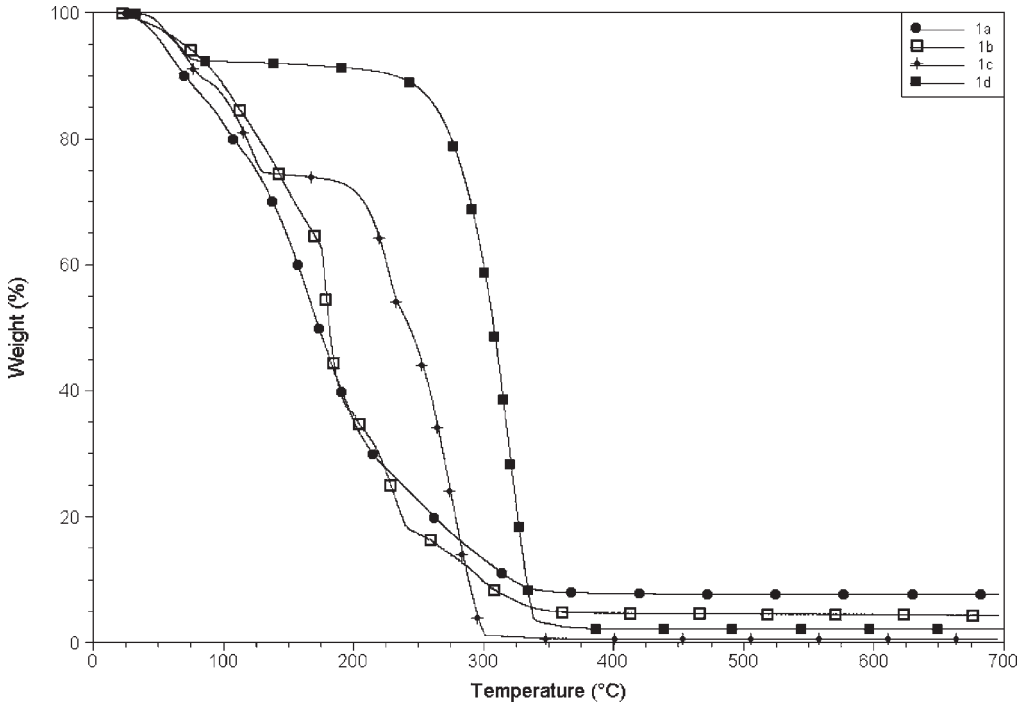

Figure 6. Thermogravimetric plot of the weight percent change for $[Mg(PFTB)_2(thf)_2]$ (**1a**), $[Ca(PFTB)_2(thf)_4]$ (**1b**), $[Sr(PFTB)_2(thf)_4]$ (**1c**), and $[Ba(PFTB)_2(thf)_4]$ (**1d**).

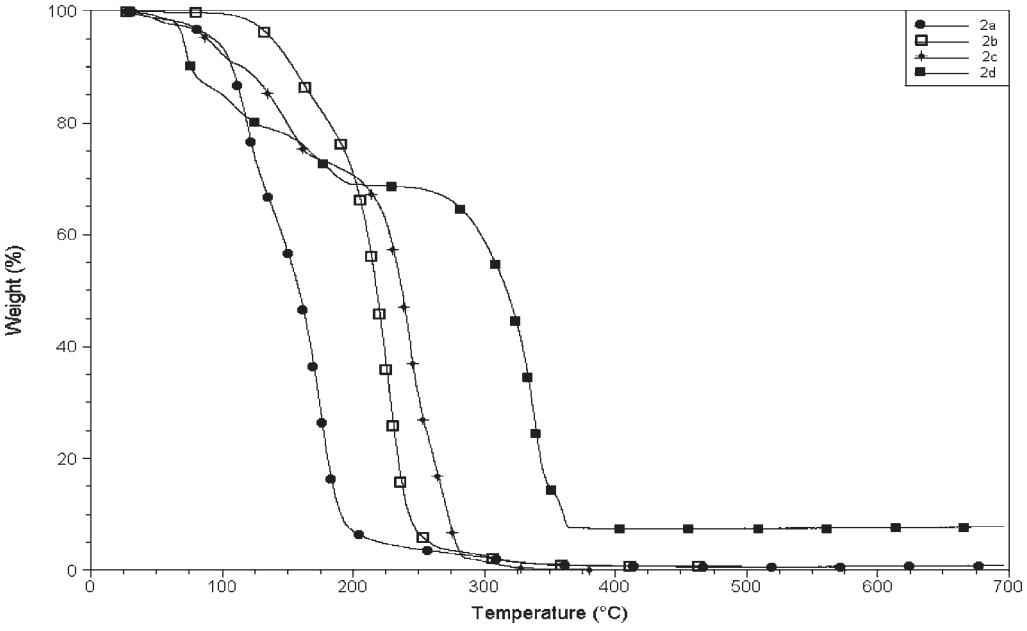

Figure 7. Thermogravimetric plot of the weight percent change for $[Mg(PFTB)_2(dme)]$ (**2a**), $[Ca(PFTB)_2(dme)_2]$ (**2b**), $[Sr(PFTB)_2(dme)_2]$ (**2c**), and $[Ba(PFTB)_2(dme)_3]$ (**2d**).

trans ligand configuration in **2d** does not allow for steric flexibility resulting in the absence of long distance Ba−F contacts.

4.2.3. Diglyme Adducted Complexes. Incorporation of the tridentate diglyme ligand affords $[Ae(PFTB)_2(diglyme)_2]$ [Ae = Ca, (**3b**); Ae = Sr, (**3c**); Ae = Ba, (**3d**)]. Coordinately **3b**−**d** are related to **2d** by the *trans* conformation of the PFTB ligand, as well as co-ligands that form a tilted belt around the metal center. Both **3c** and **3d** have a coordination number of eight forming distorted hexagonal-bipyramid geometries about the metal center (Figures 4, 5). Both **3c** and **3d**, like **2d**, have a center of symmetry located at the metal resulting in a *trans* angle of 180°; an additional similarity results from the tilted orientation of the co-ligands in **3c**−**d** to form a tilted belt around the metal center where the maximum off equatorial plane tilt is 12.8° for $Sr(PFTB)_2(diglyme)_2$ (**3c**) and 14.1° for $Ba(PFTB)_2(diglyme)_2$ (**3d**). The increase in coordination number in **3c** results in slight elongation of the Sr−O(diglyme) bonds [**3c**: Sr−O(diglyme), 2.72(4) Å (av); Table 4] compared to **1c** and **2c** [**1c**: Sr−O(THF), 2.56(6) Å (av); **2c**: Sr−O(DME), 2.58(2) Å (av)]. The Ba−O(diglyme) distance [2.86(2) Å

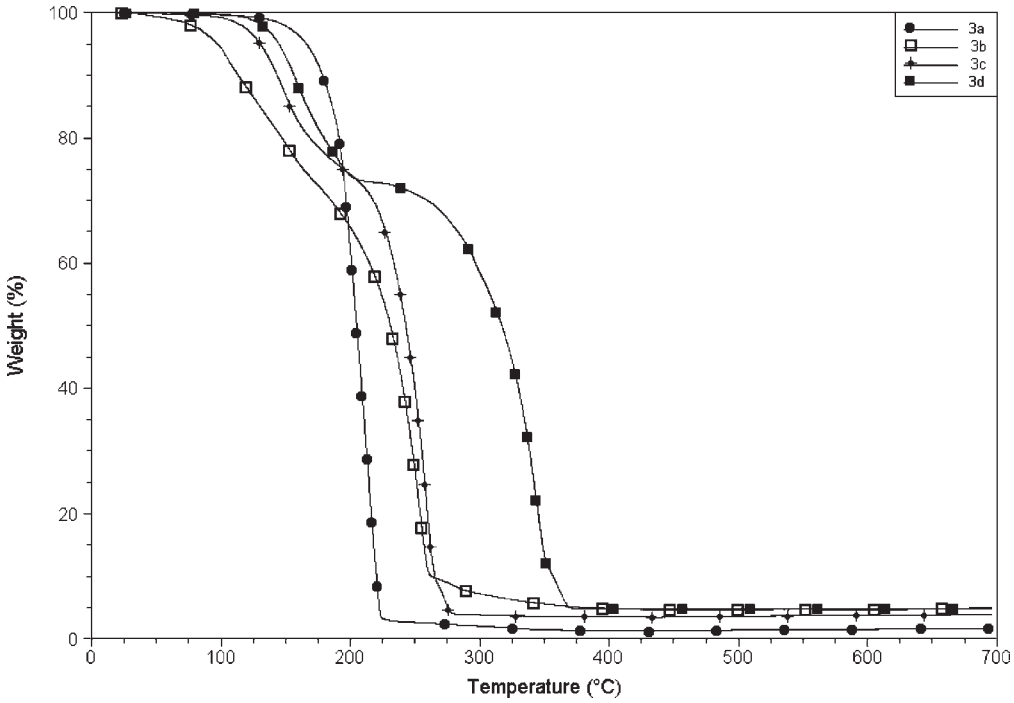

Figure 8. Thermogravimetric plot of the weight percent change for $[Mg(PFTB)_2(diglyme)]$ (**3a**), $[Ca(PFTB)_2(diglyme)_2]$ (**3b**), $[Sr(PFTB)_2(diglyme)_2]$ (**3c**), and $[Ba(PFTB)_2(diglyme)_3]$ (**3d**).

(av)] in **3d** compares well to the Ba−O(DME) distance in **2d**.

Of the diglyme species, $[Ca(PFTB)_2(diglyme)_2]$ (**3b**) varies the most in comparison to its heavier analogues. Unlike **3c**−**d** and **2d** the *trans* angles does not lie across a center of symmetry giving the O(PFTB)−Ca−O(PFTB) a modest range of 172.51(9) and 174.74(9)° for the two independent molecules. The smaller ionic radii of calcium allows **3b** to achieve coordinative saturation via seven Ca−O bonds, two to the ligand oxygen atoms and five to oxygen atoms from the diglyme co-ligand, resulting in a distorted pentagonal-bipyramid geometry on each calcium atom. The odd coordination number is possible by two of the three oxygen atoms from one diglyme interacting, while in the second one all three oxygen atoms interact with Ca. The degree of off equatorial plane tilt is 12.3°, comparing well to both **3c**−**d**. The increase in coordination number does not result in a significant increase in the Ca−O(diglyme) distances [2.49(3) Å (av)] compared to **1b** or **2b**.

4.3. Thermal Gravimetric Analyses (TGA). Thermal gravimetric analysis of the compounds discussed above reveal the high volatility of this family of compounds. All of the compounds volatilize significantly below 400 °C and, with few exceptions, leave a weight percent residue that is significantly less than the weight percent of an alkaline earth fluoride or oxide, both likely thermal decomposition products (see Table 5). The low weight percents strongly indicate that metal transport occurs and that many of these compounds have potential as precursor molecules in MOCVD. Importantly, the presence of co-ligands vastly improves the thermal properties of the compounds as the previous co-ligand free molecules required a significant vacuum ($< 10^{-5}$ Torr) to sublime at slightly higher temperatures.[23] Furthermore, certain co-ligands performed better than others, as outlined below. Table 6 contains a selected list of compounds that are often utilized for MOCVD applications and provides our basis of comparison.

The TGA profiles of the THF adducted compounds (see Figure 6) shows a steady decrease in mass for **1a**−**b**. The sublimation profile for **1a** indicates decomposition of the precursor into MgO and/or MgF_2, elucidating **1a** as an inappropriate candidate for MOCVD. Recent computational work provides evidence that the light alkaline earth metals (Be and Mg) would have more reactive complexes with fluorinated ligands, the result of the high charge to size ratio, leading to cleavage of the C−F bond.[34] Likewise, the profile for **1b** is similar to that of **1a** in that a steady decrease in weight percent is observed, but the low final weight percents for **1b** indicate a nearly complete sublimation with only 1.6−1.7 residual weight percent. Furthermore, the TGA profiles for **1c**−**d** show abrupt changes in weight percent indicating first the partial loss of the co-ligand THF molecules [**1c**: 133 °C; **1d**: 90 °C] followed by volatilization of the complex [**1c**: 287 °C; **1d**: 368 °C]. Compounds **1b**−**d** all display good thermal properties as shown by their low final weight percents and their competitiveness with contemporary ligands (see Table 6).

The DME adducted complexes displayed the best overall thermal properties. TGA profiles (see Figure 7) behave similarly to those of the THF complexes; the Mg and Ca species, (**2a**−**b**) show slow decreases indicating possible decomposition, but the Sr and Ba (**2c**−**d**) species display sudden declines in weight percent. Both **2c**−**d** seem to partially lose the coordinated DME co-ligand [**2c**: 180 °C; **2d**: 198 °C] and then sublime. However, unlike the THF adducted species, all the DME complexes leave weight

(34) Buchanan, W. D.; Allis, D. G.; Ruhlandt-Senge, K., manuscript in preparation.

percent residues that are significantly less than the weight percents of the fluoride or oxide decomposition products (see Table 5). The weight percents for **2a** and **2c** significantly decrease from the THF adducts, whereas **2b** and **2d** remain comparable to the THF species. Furthermore, the onset of sublimation does increase compared to the THF species, but the temperature where sublimation completion occurs decreases for **2a**−**b** and remains the same for **2c**−**d**. The less favorable thermal properties for **1a**−**b** are likely the result of the THF co-ligand; the multidentate DME co-ligand results in complexes more inert to the atmosphere.

With the exception of the magnesium species (**3a**), the diglyme coordinated complexes display good thermal properties (see Figure 8). Unlike the other magnesium compounds, **3a** shows a single sharp decrease beginning at 150 °C indicating the molecule sublimes intact leaving a 1.3−1.7 weight percent. However, **3b**−**d** sublime in two stages, the first being the loss of the coordinated diglyme co-ligand followed by the sublimation of the complex. Overall the diglyme coordinated complexes displayed similar thermal properties to the DME coordinated complexes, but left higher weight percents.

Many of the described complexes (**1c**−**d**, **2c**−**d**, and **3b**−**d**) display a two-stage sublimation profile where initially the bound co-ligand is lost followed by sublimation of the complex. This indicates that the co-ligand is necessary as it prevents initial aggregation of the alkaline earth species. During heating the loss of co-ligand does not allow for extended aggregation to occur (likely through M−F and extend bridging motifs) and thus the complexes retain the sought after volatility. Established compounds display higher sublimation points;[23] possibly the result of extended aggregation thus decreasing the volatility of these compounds. Furthermore, the DME co-ligand seems to optimize the thermal properties for many of these compounds (**2a**, **2b**, **2c**), with the ligands' bidentate nature providing enough steric saturation for the metal centers to make the complexes inert for safe handling, yet DME is removed easily under heating without raising the sublimation point too high. This is demonstrated in Table 5 where both sublimation onset and completion are shown to compare favorably to the other complexes reported here as well as to previously reported complexes. Furthermore, the low weight percents for the DME coordinated compounds indicate a minimal amount of residue, suggesting near quantitative sublimation for many of the reported complexes.

5. Conclusion

A series of alkaline earth PFTBs has been prepared and evaluated for its potential as a MOCVD precursor. The success of this ligand with alkaline earth metals can be explained by the large steric bulk (reducing oligomerization), and the use of co-ligand molecules which further decrease oligomeric tendencies. Complexes containing one of the co-ligands THF, DME, or diglyme significantly increased the volatility of the complex when compared to the previous co-ligand free species.[22,23] Additionally, several synthetic strategies were developed that allow the isolation of high quality products with very short reaction times (1−18 h).

The complexes of this study have shown exceptional stability toward air unlike other MOCVD precursors. The resulting complexes not only show excellent thermal gravimetric profiles, but exposure to atmospheric conditions (O_2/H_2O) does not lead to pyrophoric decomposition of the materials illustrating a significant increase in safety.

A series of novel, volatile alkaline earth complexes containing PFTB as the ligand has been examined. The facile preparation of these complexes was achieved utilizing the metals and using liquid ammonia to activate the metals. This route enabled the synthesis of high yield and purity products. Furthermore, co-ligands could easily be exchanged (THF to DME, or THF to diglyme) tuning the thermal properties to more desirable sublimation onsets and significantly decreasing the residue weight percents. Single crystal X-ray analyses of these compounds reveals a series of monometallic compounds where the bulky PFTB ligand occupies either the *cis* or the *trans* position in octahedral or pseudo-octahedral environments around the metal centers. The co-ligands allow monomeric complexes with excellent thermal properties. The DME co-ligand seems to optimize the thermal properties for Ca and Sr.

Acknowledgment. The authors gratefully acknowledge support from the National Science Foundation (CHE 0753807). Purchase of the X-ray diffraction equipment was made possible with grants from the National Science Foundation (CHE-9527858 and CHE-0234912), Syracuse University, and the W. M. Keck Foundation.